Magnetic Near-Field Measurements Over LSI Package Pins by Fiber-Edge Magnetooptic Probe

Mizuki Iwanami, Etsushi Yamazaki, Ken Nakano, Toshio Sudo, *Senior Member, IEEE*, Shigeki Hoshino, Shinichi Wakana, *Member, IEEE*, *Member, OSA*, Masato Kishi, and Masahiro Tsuchiya, *Member, IEEE*

***Abstract*—To establish a method for investigating hidden radiation sources and their mechanisms in a printed circuit board, we performed preliminary measurements of one-dimensional magnetic near-field distribution over pins of a large-scale integrated circuit (LSI) package by means of an optical method: the fiber-edge magnetooptic (FEMO) probing technique. The FEMO probe consists of fiber optics and a magnetooptic crystal glued at a fiber edge. Its planar spatial resolution is approximately 100 μm. It was found that a magnetic field generated from each LSI pin could be distinguished and some radiation was generated from ground and power supply lines. We compared the measured results with corresponding radiated electric field strength that was separately measured. The frequency of interest was the tenth harmonic of the output signal. We observed a strong correlation between those two experimental results, which suggests the effectiveness of our proposed method for near-field investigation. One of the beneficial features of the FEMO probe is its small probe head, due to which one can perform detailed near-field evaluations in a microscopic region. Furthermore, we tried to specify a major electromagnetic interference source by additional measurements of near-field distributions and frequency dependence of magnetooptic signals. It was suggested that the short-through current flowing in the power-supply system of the input/output circuits caused high-level radiated emission.**

***Index Terms*—Electromagnetic interference (EMI) source, fiber-edge magnetooptic (FEMO) probing technique, large-scale integrated circuit (LSI) operation mode, LSI pins, magnetic near-field distribution, radiated electric field strength.**

I. INTRODUCTION

ELECTROMAGNETIC near-field probes that utilize optical measurement techniques have attractive features such as low invasiveness and wide bandwidth [1]–[3]. They have been mainly applied for performance or failure diagnosis of microwave circuits with a relatively simple structure and are appreciated as efficient tools for near-field mapping. However, their potential for near-field characterization of an active device, particularly that associated with electromagnetic interference (EMI), has been rarely demonstrated until now.

With increasing operation speed and packaging density of electronic devices, the EMI problems in electronic equipment become more and more serious. It is considered that the product of all of the following factors can generally express the strength of EMI:

1) intensity of a signal which is responsible for EMI in a generation source;
2) transmission coefficient for a signal channel;
3) radiation efficiency of an unintended antenna causing EMI.

Typically, a generation source is large-scale integrated circuit (LSI) [4], [5]. There are several objects that can become a resultant signal channel, for example, leads of an LSI package and power/ground layers in a printed circuit board (PCB). Power/ground layers in a PCB as well as cables attached to electronic equipment can also become an unintended antenna [6].

Recently, with the growing complexity of circuits, it has become highly desirable to prevent the problems in the early stages of design and packaging of electronic components. To conform to such a trend, it is indispensable to evaluate the correlation between electromagnetic near-field distribution and radiated emission and to find out hidden EMI sources. Hence, the near-field probing technique with high spatial resolution and wide bandwidth is needed for realizing this purpose [7]–[9].

The electrooptic probing has been successfully utilized for characterization of electric near-fields [1]. However, one should note that a magnetic near-field is more directly associated with a current than an electric near-field, and an origin of radiated emission from radiators is known to be a radio-frequency (RF) current. Therefore, it is considered more essential to apply the magnetooptic (MO) probing technique in the evaluation of EMI generation sources.

Near-field scanning optical microscopy utilizing a MO effect is known to be a powerful MO probing technique with very high spatial resolution [10], [11]. Although it has been widely used for characterizing static magnetic fields, it is not intended to detect wide-band radiated fields, and thus it is inadequate for our purpose.

We believe that the fiber-edge magnetooptic (FEMO) probing technique that is used in this paper promises to meet the requirement described above. It consists of fiber optics and a MO

Manuscript received April 28, 2003; revised August 13, 2003. This work was performed in part under the management of ASET in the basic plan of Research and Development on Ultra High-Density Electronics System Integration supported by New Energy and Industrial Technology Development Organization.

M. Iwanami, K. Nakano, T. Sudo, and S. Hoshino are with the Association of Super-Advanced Electronics Technologies, Tsukuba Center Inc., Tsukuba, 305-0047 Ibaraki, Japan (e-mail: iwanami@si3d-aset-unet.ocn.ne.jp).

E. Yamazaki was with the Department of Electronic Engineering, University of Tokyo, Tokyo 113-8656, Japan. He is now with Network Innovation Laboratories, NTT, Yokosuka 239-0847, Japan.

S. Wakana was with the Department of Electronic Engineering, University of Tokyo, Tokyo 113-8656, Japan. He is now with Fujitsu Laboratories Ltd., Atsugi 243-0197, Japan.

M. Kishi is with the Department of Electronic Engineering, University of Tokyo, Tokyo 113-8656, Japan.

M. Tsuchiya was with the Department of Electronic Engineering, University of Tokyo, Tokyo 113-8656, Japan. He is now with the Communications Research Laboratory, Tokyo 184–8795, Japan.

Digital Object Identifier 10.1109/JLT.2003.820047

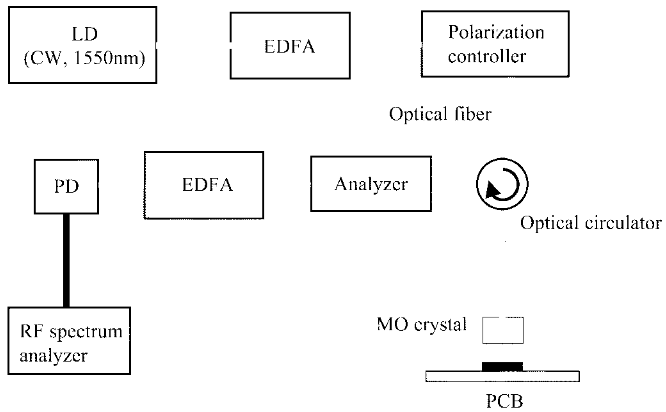

Fig. 1. Schematic diagram of a probing system for magnetic near-field measurements.

crystal glued at a fiber edge [2]. In addition to its low invasiveness, the structure can be fabricated to have high spatial resolution [12] or wide bandwidth [3].

To investigate the correlation between magnetic near-field and radiated emission in the LSI-mounted PCB, we measured one-dimensional (1-D) magnetic near-field distribution over LSI package pins by means of the FEMO probing technique. It was found that the FEMO probe could distinguish a magnetic field generated from each of the LSI pins with a width of 200 μm and an interval of 500 μm. We compared the measured results with corresponding radiated electric field strength separately measured in an anechoic chamber. We confirmed there was a strong correlation between those two experimental results. Furthermore, through additional measurements of near-field distributions and frequency dependence of magnetooptic signals, we discussed a generation source of EMI.

II. Probing System

Fig. 1 shows a schematic diagram of a probing system for magnetic near-field measurements. It consists of the FEMO probe head and its optical system [2], [3], [12]. All apparatuses in the optical system are connected by optical fibers. The 1550-nm continuous-wave (CW) light emitted from a semiconductor laser diode (LD) passes through an Er-doped fiber amplifier (EDFA), a polarization controller, and an optical circulator, and is launched from the edge of a core-expanded fiber into the MO crystal. The incident light in the MO crystal is reflected by a high-reflection dielectric mirror on the bottom surface and reenters the optical fiber. During one round-trip in the crystal, the light responds to the magnetic field surrounding a device under test (DUT) through the MO effect and its polarization is modulated. The polarization modulation is converted into intensity modulation through an analyzer. After the compensation of optical loss caused in the fiber optics and the MO crystal, the light is converted to electrical signals by a photodetector (PD). The RF photocurrent detected by a RF spectrum analyzer is regarded as the MO signal. Therefore, because the intensity of the MO signal responds to that of the external magnetic field, a magnetic near-field distribution is obtained by scanning the probe head over a DUT. The MO crystal glued at the edge of an optical fiber is

TABLE I
Specifications of a Test LSI

Process	0.35 μm, 2 level metal layers
Design	CMOS gate array
Chip size	9.95 x 9.95 mm
Package	Quad Flat Package (QFP)
Number of pins	304
Width/interval of package pins	200 μm/500 μm
Power supply	Separation of I/O V_{DD} from Core V_{DD}

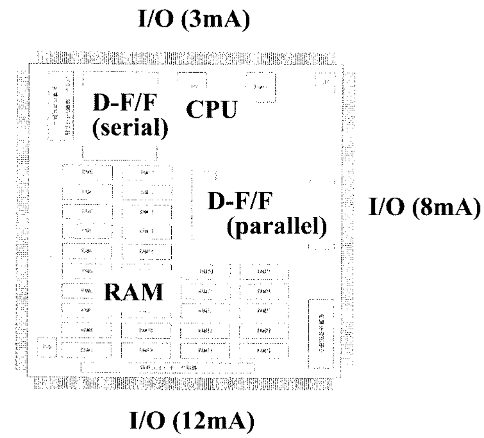

Fig. 2. Circuit configuration of a test LSI.

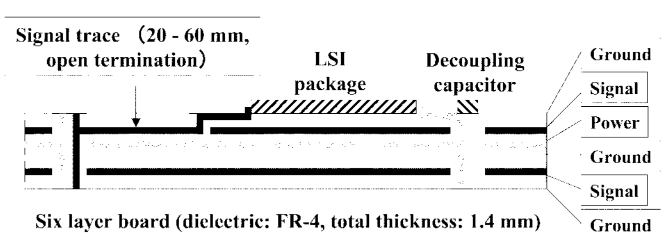

Fig. 3. Side view of a fabricated PCB.

bismuth-substituted rare-earth iron garnet (BiRIG). The size of the crystal is 400 $\times$ 400 μm^2 in area $\times$ 240 μm in height. The spatial resolution of the FEMO probe utilized for near-field distribution measurements is approximately 100 μm [14].

III. Test LSI and PCB

A test LSI and a PCB have been developed for evaluating the effect of LSI operation mode on EMI [13]. In the developed LSI, the operation modes can be controlled from the outside. The specifications of a test LSI are shown in Table I. It has been fabricated in a complimentary metal–oxide–semiconductor (CMOS) gate array with 0.35-μm process technology. The chip size was 9.95 $\times$ 9.95 mm^2. The LSI was housed in a conventional quad flat package (QFP) with 304 pins with a width of 200 μm and an interval of 500 μm. Fig. 2 shows a circuit configuration of a test LSI. It consisted of the central processing unit (CPU), random access memory (RAM), interface circuits for external control, and noise-generating circuits. Both

TABLE II
LSI OPERATION MODES FOR EVALUATIONS

LSI operation mode	Circuit operation	Frequency of internal clock	Frequency of output data	Output voltage for traces
Test circuit idle	CPU, clock & data generators	25.5 MHz	Non	Non
Internal circuit operation	D-F/F	25.5 MHz	12.75 MHz	Non
I/O circuit operation (12 mA)	12 mA I/O	25.5 MHz	12.75 MHz	3.3 V/0 V (Rectangle, 12.75 MHz)
I/O circuit operation (3 mA)	3 mA I/O	25.5 MHz	12.75 MHz	3.3 V/0 V (Rectangle, 12.75 MHz)

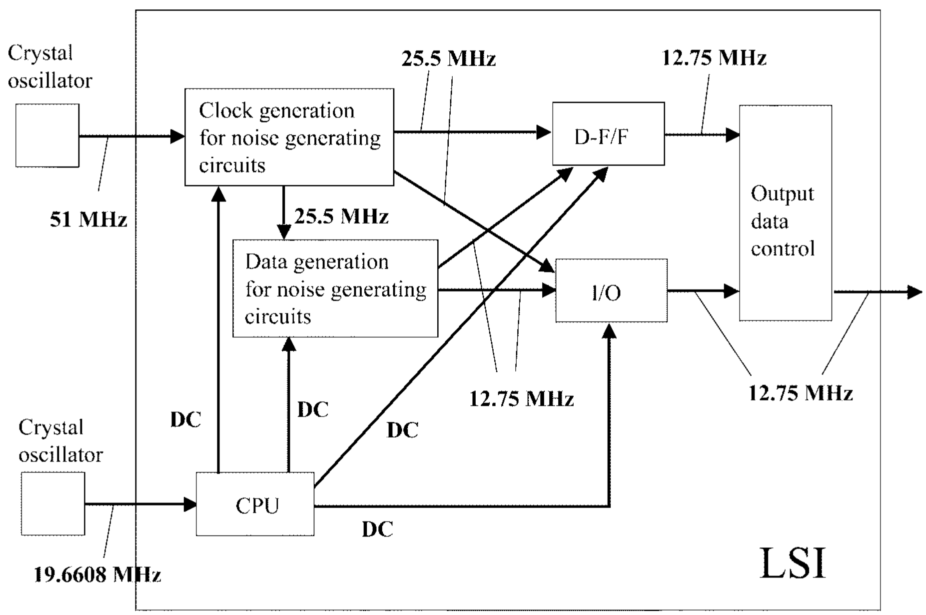

Fig. 4. Block diagram of LSI operations.

input/output (I/O) buffer circuits and internal logic circuits were designed as noise-generation sources. The I/O buffer circuits consisted of CMOS drivers with three different current drivabilities: 3-mA driver, 8-mA driver, and 12-mA driver.

Each driver has 48 buffers and was allocated at a side of the chip as shown in Fig. 2, that is, a total of 144 I/O buffers were incorporated on the periphery of the test LSI. Two types of logic circuits—D-type flip-flop (D-F/F) circuits and buffer chain circuits—were incorporated as internal logic circuits. To avoid the interaction inside the chip, a separated power-supply system (that consists of separated power layers and a common ground) was adopted for the I/O buffer circuits and the internal logic circuits.

An evaluation board for mounting the LSI package was designed. Its planar size was 180 $\times$ 180 mm^2. Fig. 3 shows a side view of a fabricated PCB. It consisted of six conductive layers with a dielectric (FR-4) between each of them. The top and bottom layers were ground planes. Signal layers were provided as the second and fifth layers, which are next to the ground planes. A power layer that is commonly used to supply power to the I/O buffer and the internal logic circuits was allocated as the third layer. Clocks for the CPU (19.6608 MHz) and noise-generating circuits (51 MHz) were provided by crystal oscillators mounted on the PCB.

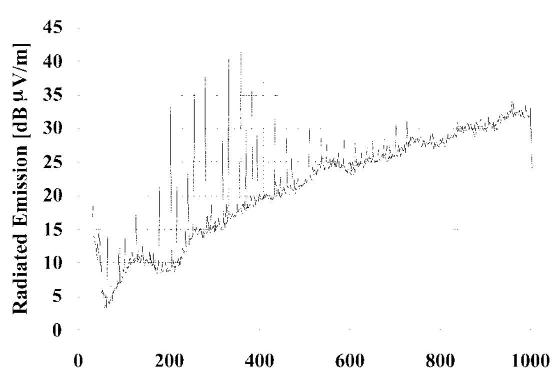

Fig. 5. Radiated electric field strength for 12-mA I/O circuit operation mode (vertically polarized wave).

TABLE III
RADIATED ELECTRIC FIELD STRENGTHS AT 127.5 MHz

	Antenna height 1 m		Antenna height 2 m	
	Horizontally polarized wave [dBuV/m]	Vertically polarized wave [dBuV/m]	Horizontally polarized wave [dBuV/m]	Vertically polarized wave [dBuV/m]
Test circuit idle	2.5	2.5	2.5	2.5
Internal circuit operation (D-F/F)	6	5	6	8
I/O circuit operation (12 mA)	15	9	18	14
I/O circuit operation (3 mA)	12.5	9.5	15	15.5

IV. RADIATED ELECTRIC FIELD STRENGTH

To investigate a correlation between radiated emission and magnetic near-field, we selected four kinds of LSI operation modes as shown in Table II. For understanding of each operation, a simplified block diagram of LSI operations is shown in Fig. 4. In both cases of the test circuit idle and internal circuit operation modes, there is no signal output for traces connecting with the LSI pins. When the I/O circuit operation mode is selected, the rectangular output voltages that have a 180° phase difference with respect to adjacent traces are transmitted.

Fig. 5 shows the radiated electric field characteristic of the PCB measured in an anechoic chamber. The horizontal distance between the PCB and the antenna was 3 m and their heights from the chamber floor were 0.8 and 2 m, respectively. The LSI operation mode was 12-mA I/O circuit operation, which showed the highest emission level among four kinds of LSI operation modes. High-level emissions are observed in the frequency range from 200 to 500 MHz. It should be noted that those frequencies are even multiples of 12.75 MHz, the fundamental of the output signal. Although it is very interesting to measure the magnetic near-field distribution in this frequency range, the FEMO probe used in this study did not have sufficient sensitivity for measurement. Therefore, we have systematically investigated the radiation strength for the LSI operation modes in Table II at 127.5 MHz, which is tenfold that of the fundamental of the output signal. Using a field strength meter, we measured the radiation strengths of both horizontally and vertically polarized waves with the conditions of antenna heights of 1 and 2 m. Table III shows the measured result. We can find that the radiation levels in the cases of I/O circuit operation modes are higher, and in particular, the maximum strength is observed for the 12-mA I/O mode in the case of both antenna heights. To investigate the origin of the differences in the radiation strengths, we tried to measure magnetic near-field distributions over peripheral pins of the LSI package.

V. MAGNETIC NEAR-FIELD DISTRIBUTION OVER PINS OF LSI PACKAGE

Fig. 6 shows the configuration of the FEMO probe head to the DUT for magnetic near-field distribution measurements. The gap between the probe head and LSI pins was set to be approximately 50 μm and the probe head was one-dimensionally scanned with a pitch of 50 μm. When we measure the magnetic near-field in the configuration of Fig. 6, the probe detects the field element perpendicular to a surface of a DUT [2], [12]. In the case of the I/O circuit operation mode, the measurement was carried out over the corresponding LSI pins. On the other hand, measurements for other operation modes were performed over the pins for the 3-mA I/O circuit (see Fig. 2).

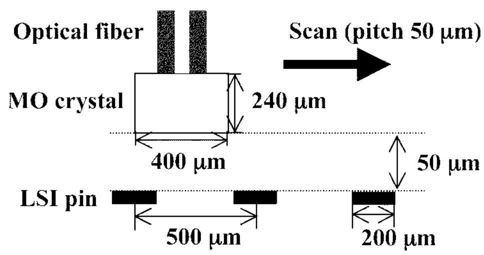

Fig. 6. Configuration of the FEMO probe head to the DUT for magnetic near-field distribution measurements.

Fig. 7 shows measured results of one-dimensional (1-D) magnetic near-field distribution at 12.75 MHz. The profiles of MO signals were normalized to the maximum value. In the results for the test circuit idle and internal circuit operation modes, no peaks were observed, while in both cases of the I/O circuit operation modes, sharp peaks appeared continuously. It was found that these peaks were located between two adjacent pins. As a result, we could identify which pin contributed to each magnetic peak. In Fig. 7(c), for example, it was found that most peaks that had their intensities at above −5 dB, resulting from the magnetic fields generating from the pins for I/O. Smaller peaks were due to the magnetic fields from the pins for power or ground.

The 1-D magnetic near-field distributions at 127.5 MHz are shown in Fig. 8. Note that these profiles and those shown later were normalized to the maximum value in Fig. 7(c) and were corrected by adding an amount of lowering of the probe sensitivity. As a result, one can directly compare the peak intensities among the profiles at the same or different frequency. Again, peaks were observed in both profiles of the I/O circuit operation modes. It was confirmed that all peaks were due to the magnetic fields from the pins for power or ground. One should note that the peaks in Fig. 8 are larger than those caused by the fields from the power/ground pins in Fig. 7. It can be seen that the radiation for the 12-mA I/O mode is stronger than that for the 3-mA I/O mode. From a comparison between Fig. 8 and Table III, we can confirm the strong correlation, that is, the I/O

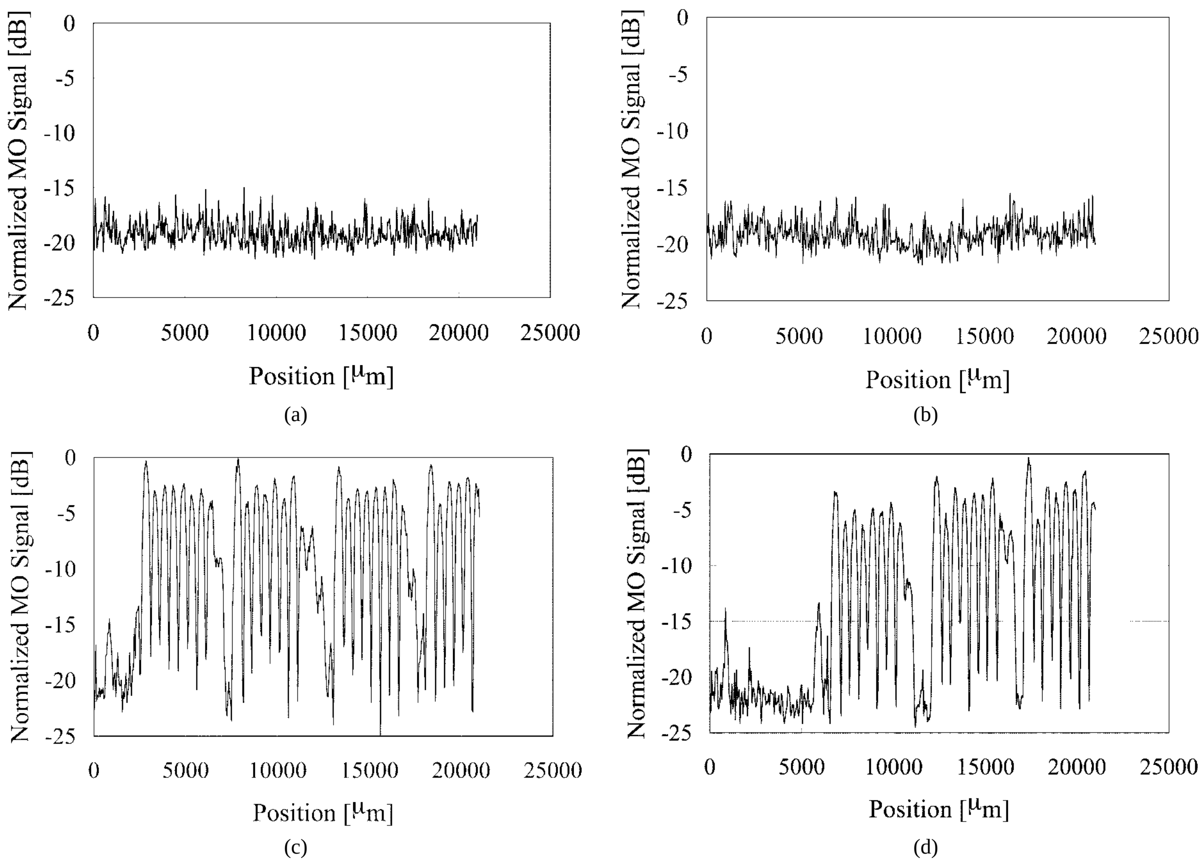

Fig. 7. 1-D magnetic near-field distributions over LSI pins at 12.75 MHz, (a) test circuit idle, (b) internal circuit operation, (c) 12-mA I/O circuit operation, (d) 3-mA I/O circuit operation.

circuit operation mode gives a higher radiation level in the case of both magnetic near-field and electric far-field. The measured results of magnetic near-fields suggest that the difference of radiation strengths in Table III resulted from that of radiation level in the power-supply system, which means that the power supply system of the I/O circuits has a great potential as the EMI generation source. Furthermore, these results also demonstrate that the FEMO probing technique can become an effective tool for near-field investigation of electronic devices.

VI. Discussion on the EMI Generation Source

In this section, we discuss a generation source of EMI on the basis of measured results of near-field distribution and frequency dependence of MO signals.

In [5], it was demonstrated that a high-frequency current generated in a power-supply system of LSI caused EMI from a PCB that had a simple structure with power and ground planes and no signal trace. As mentioned above, the power-supply system of the I/O circuits has a high possibility as the EMI source in our evaluation board. As is well known, in CMOS circuits a transient current flows in power and ground lines when an output voltage is rising or falling [13], [15]. The transient current is classified into two types: the charge–discharge current and the short-through current. The latter flows between power and ground lines when both transistors instantaneously switch on during the high-to-low or low-to-high transition and is known as the origin of the so-called delta-I or switching noise [6]. Therefore, it could be speculated that either or both currents contributed to the peaks in Fig. 8. In general, the effects of these currents on power-supply lines are indirectly evaluated all together by measuring the voltages of boards in the time domain [13], [18]. We considered that if those peaks were caused by the short-through current, by applying the FEMO probe, there was a possibility of verifying it based on the following reasoning. The charge–discharge current is considered to have the same frequency components as an output current, since they are essentially equivalent and form a loop around signal and power/ground lines [15]. Hence, its fundamental should be the same as that of an output current, in this study, 12.75 MHz. On the other hand, in the case of the short-through current, it can be considered that its fundamental is once or twice that of an output voltage, which depends on the current waveform during rising and falling of an output voltage. These contents mean that if the fundamental of the current generating the peaks in Fig. 8 is 25.5 MHz, the origin of the peaks is the short-through current. Therefore, first, we attempted to identify the type of the current by investigating its fundamental. We measured the magnetic near-field distributions at 25.5 and 114.75 MHz, the ninth harmonic of the output signal. Here, the reason for the measurement at 114.75 MHz is as follows. If the fundamental of the current was 12.75 MHz, the ninth harmonic peaks by that should also be observed. Figs. 9 and 10 show the measured results. All peaks in Fig. 9 were found to result from the magnetic fields generated from the pins for power or ground. On the other hand, there is no peak in Fig. 10. These results suggest that the peaks

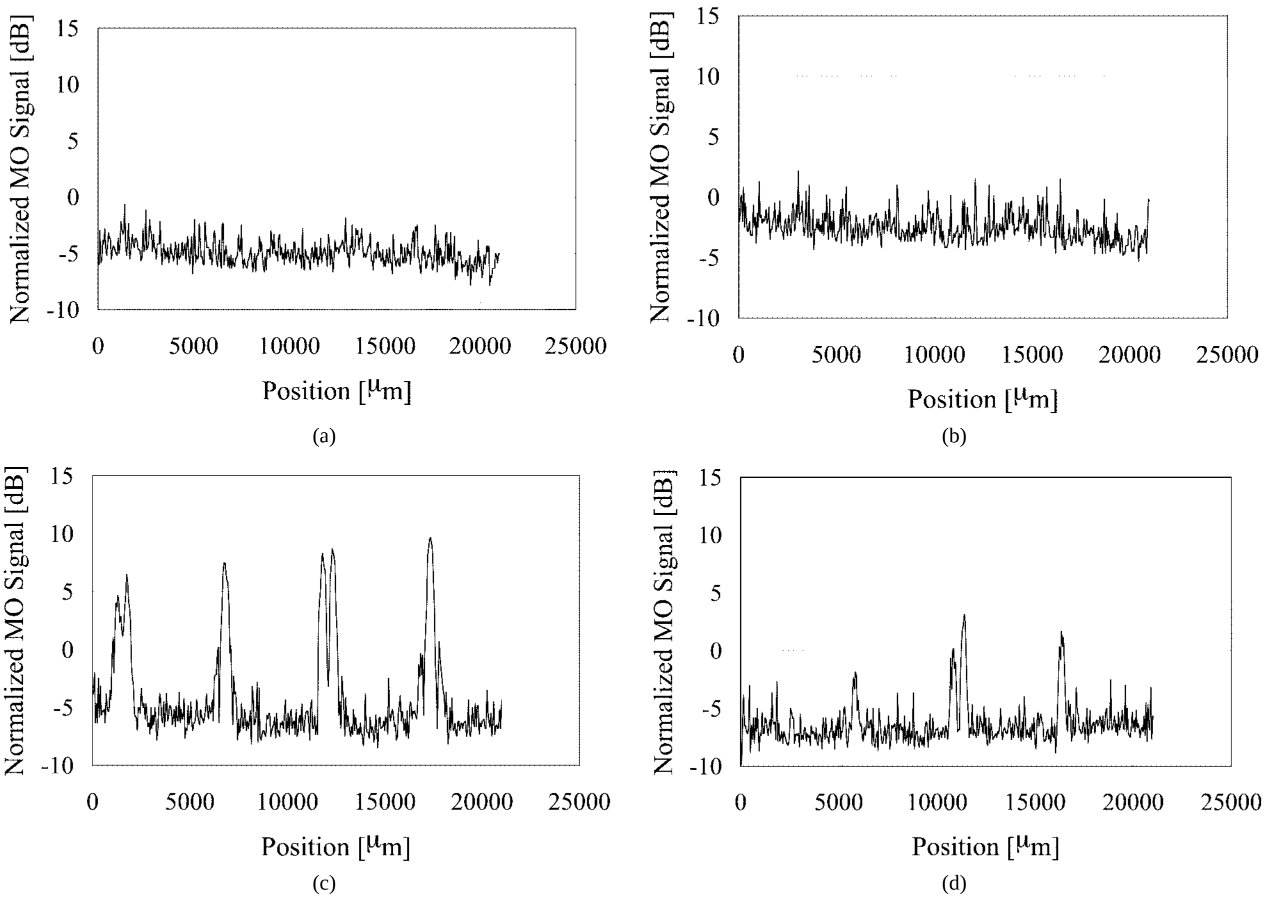

Fig. 8. 1-D magnetic near-field distributions over LSI pins at 127.5 MHz: (a) test circuit idle, (b) internal circuit operation, (c) 12-mA I/O circuit operation, and (d) 3-mA I/O circuit operation.21jlt12-iwanami

observed at 127.5 MHz [Fig. 8(c) and (d)] were caused by the harmonic of the short-through current.

Next, we attempted to investigate the correlation between frequency dependences of the magnetic near-field and electric far-field strengths. In the measured result of radiated electric field (Fig. 5), the frequencies at which high-level emissions were observed were even multiples of 12.75 MHz. We considered that it is important to specify which system between power supply and I/O causes this feature. Fixing the probe at the position between LSI pins, we measured the frequency dependence of MO signals. For the measurements, we used a new type of FEMO probe with a wide bandwidth, which employs the Faraday effect during rotations of magnetization of an MO crystal [3]. Its measurable bandwidth is over 10 GHz with the sensitivity of minimum detectable current of 140 μA [3]. The MO signals were measured between power and ground pins or I/O pins with a gap of approximately 1 μm. The frequencies of interest were multiples of 12.75 MHz. The measured result is shown in Fig. 11, where circular and triangular dots represent the MO signal intensities between power and ground pins and between I/O pins, respectively. In the case between power and ground pins, signal intensities at 12.75 $\times$ $2n$ MHz are higher than those at 12.75$\times$ $(2n{+}1)$ MHz, where n is an integer. From the discussion described above, we believe that the short-through current almost contributes the entire signal intensity at 12.75 $\times$ $2n$ MHz and the charge-discharge current generates that at 12.75$\times(2n{+}1)$ MHz. On the other hand, the case between I/O pins shows a contrary characteristic, i.e., signal intensities at 12.75 $\times$ $2n$ MHz are lower. One should note that intensities of high-level MO signals are larger for the former, and the relationship between the signal intensities of the two is consistent with the measured results for near-field distribution. Although the frequency band is different, the MO signal characteristic measured between power and ground pins has the same feature as the electric field strength characteristic. This suggests that the emission from the power supply system resulted in the feature of the electric far-field, that is, the origin of the high-level emission was a current flowing in the power-supply system.

From the results and discussions described above, it can be considered that the major EMI source of our evaluation board is the short-through current flowing in the power-supply system of the I/O circuits. Although detailed evaluations to verify this consideration are future work, we would like to emphasize that such knowledge could not be obtained until one performed frequency-domain measurements by means of a highly efficient magnetic near-field probing technique.

Unfortunately, because of insufficient probe sensitivity, we could not measure the MO signal characteristic above 300 MHz. However, it can be speculated from Fig. 11 that a smaller amount of currents into the power-supply system result in the high-level emission from the PCB, since the probe sensitivity negligibly changes, to around 10 GHz [3]. Finally, we examine this possibility.

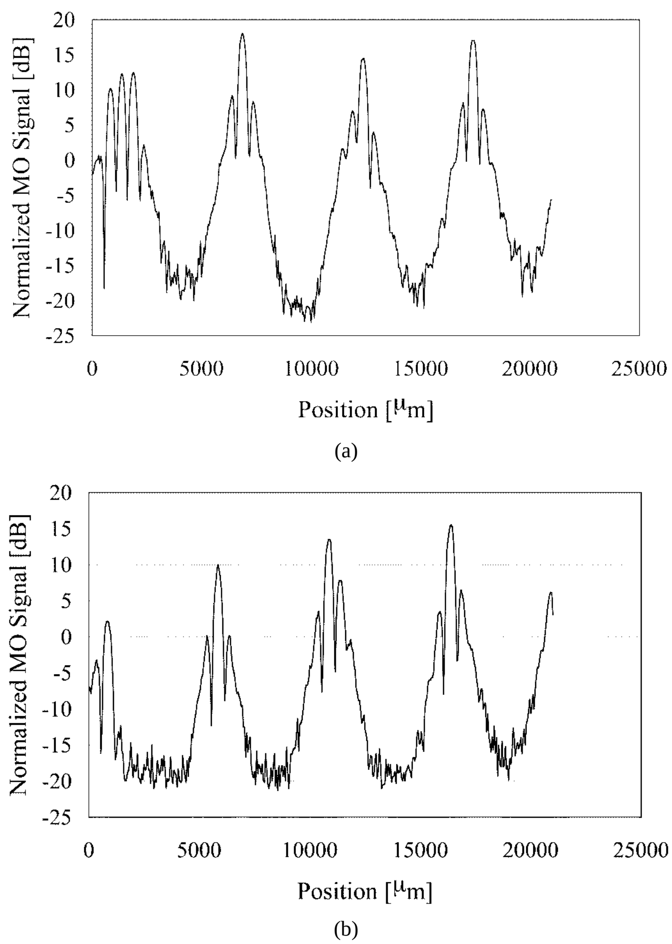

Fig. 9. 1-D magnetic near-field distributions over LSI pins at 25.5 MHz: (a) 12-mA and (b) 3-mA I/O circuit operation.

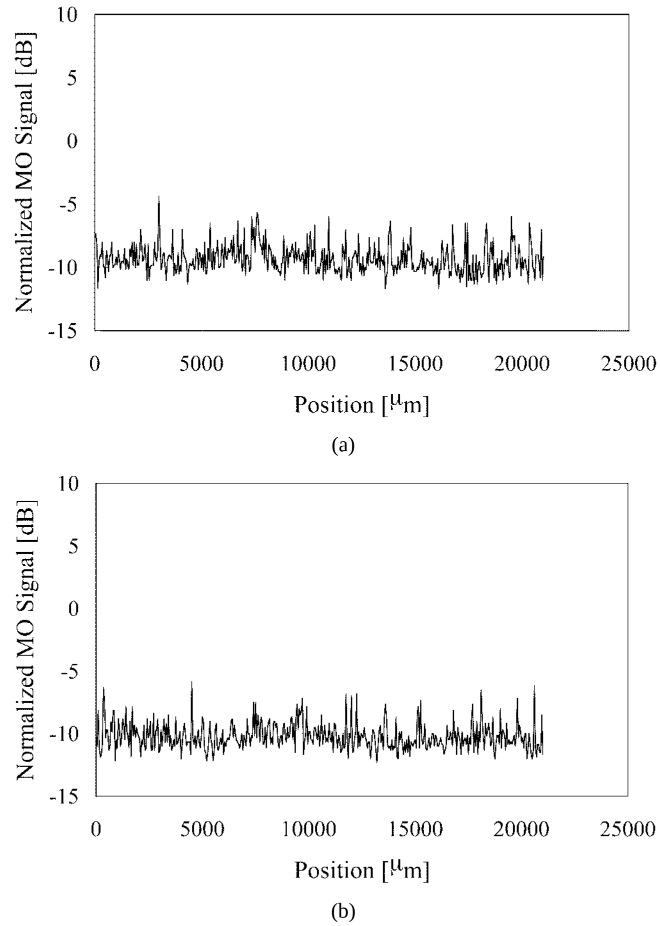

Fig. 10. 1-D magnetic near-field distributions over LSI pins at 114.75 MHz: (a) 12-mA and (b) 3-mA I/O circuit operation.

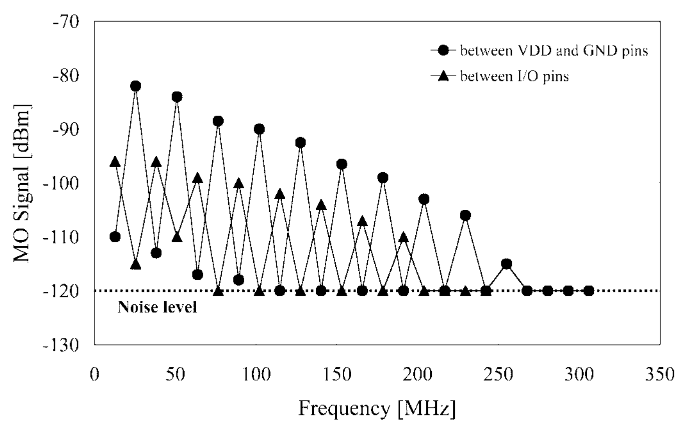

Fig. 11. Frequency dependence of MO signals measured at the position between LSI pins (12-mA I/O circuit operation).

It is known that the resonance that occurs in a power-supply system of a PCB leads to strong emission, and several authors reported a strong correlation between a resonance peak in the transmission coefficient ($|S_{21}|$) characteristic of that and high-level emission [16], [17]. In [16], it is demonstrated that at resonance frequencies, standing waves with high amplitude arise in a power-supply system, which means that the system behaves as an antenna with high radiation efficiency. Therefore, using a conventional network analyzer, we measured $|S_{21}|$ of the power-supply system of the PCB. Two semirigid coaxial cables were soldered to the power and ground pads connected with those layers at the opposite corners of the PCB. The measured $|S_{21}|$ is shown in Fig. 12. One can find the resonance peaks in the frequency range from 200 to 500 MHz in which the high-level emission was observed. We believe from this result that the power-supply system of our evaluation board could become a resonator with high radiation efficiency in this frequency range, which led to the high-level emission from the PCB even if the currents in the power-supply system were small. Detailed analysis of the emission mechanism will be reported elsewhere.

VII. Conclusion

In this paper, under the consideration that magnetic near-field intensity is closely associated with EMI, we investigated the correlation between them in the LSI-mounted PCB. We measured the one-dimensional magnetic near-field distribution over the pins of an LSI package by means of the FEMO probing technique. It was found that a magnetic field generated from each LSI pin could be distinguished and some radiation was generated from ground and power-supply lines. We compared the measured results with corresponding electric far-field strength at a frequency of the tenth harmonic of the output signal. We observed a strong correlation between these two experimental results and found that the power-supply system of the I/O circuits had a high possibility as the EMI source. Finally, to specify the

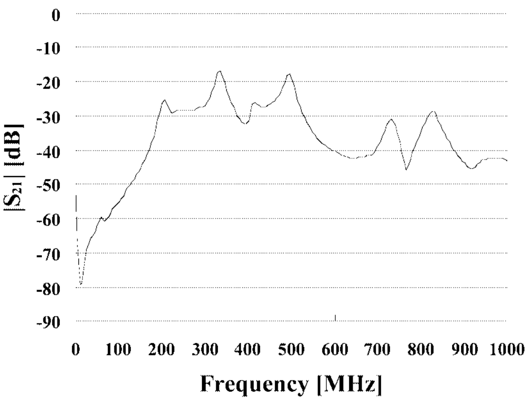

Fig. 12. $|S_{21}|$ of the power-supply system of the PCB.

EMI source, we investigated the fundamental of the current generating the harmonic peaks in the near-field distribution and the correlation between the frequency dependences of the magnetic near-field and electric far-field strengths. It was suggested that the short-through current in the power-supply system caused the harmonic peaks. What is more important, the MO signal characteristic measured between power and ground pins had the same feature as the electric field strength characteristic. From the investigations, it could be speculated that the major EMI source of our evaluation board was the short-through current flowing in the power-supply system of the I/O circuits.

These research results demonstrate that the FEMO probing technique can be an effective tool for near-field investigation and toward low-EMI designs of electronic devices.

ACKNOWLEDGMENT

M. Iwanami would like to thank H. Park, University of Tokyo, Tokyo, Japan, for his technical support.

REFERENCES

[1] K. Yang, G. David, S. V. Robertson, J. F. Whitaker, and L. P. B. Katehi, "Electrooptic mapping of near-field distributions in integrated microwave circuits," *IEEE Trans. Microwave Theory Tech.*, vol. 46, pp. 2338–2343, Dec. 1998.

[2] S. Wakana, T. Ohara, M. Abe, E. Yamazaki, M. Kishi, and M. Tsuchiya, "Fiber-edge electrooptic/magnetooptic probe for spectral-domain analysis of electromagnetic field," *IEEE Trans. Microwave Theory Tech.*, vol. 48, pp. 2611–2616, Dec. 2000.

[3] E. Yamazaki, H. Park, S. Wakana, M. Kishi, and M. Tsuchiya, "Implementation of magneto-optic probe with $>$ 10 GHz bandwidth," *Jpn. J. Appl. Phys.*, vol. 41, no. 7B, pp. L864–L866, July 2002.

[4] K. P. Slattery, J. W. Neal, and W. Cui, "Near-field measurements of VLSI devices," *IEEE Trans. Electromagn. Compat.*, vol. 41, no. 4, pp. 374–384, Nov. 1999.

[5] Y. Fukumoto, O. Shibata, K. Takayama, T. Kinoshita, Z. L. Wang, Y. Toyota, O. Wada, and R. Koga, "Radiated emission analysis of power bus noise by using a power current model of an LSI," in *Proc. 2002 IEEE Int. Symp. Electromagnetic Compatibility*, Aug. 2002, pp. 1037–1042.

[6] A. R. Djordjevic and T. K. Sarkar, "An investigation of delta-I noise on integrated circuits," *IEEE Trans. Electromagn. Compat.*, vol. 35, pp. 134–147, May 1993.

[7] Y. Gao and I. Wolff, "A new miniature magnetic field probe for measuring three-dimensional fields in planar high-frequency circuits," *IEEE Trans. Microwave Theory Tech.*, vol. 44, pp. 911–918, June 1996.

[8] ——, "Miniature electric near-field probes for measuring 3-D fields in planar microwave circuits," *IEEE Trans. Microwave Theory Tech.*, vol. 46, pp. 907–913, July 1998.

[9] N. Masuda, N. Tamaki, H. Wabuka, T. Watanabe, and K. Ishizaka, "A multilayer board-type magnetic field loop probe with high spatial resolution and RF current estimation method for ICs," in *Proc. EMC '99 Int. Symp.*, vol. S14, Tokyo, May 1999, p. 801.

[10] E. Betzig, J. K. Trautman, R. Wolfe, E. M. Gyorgy, P. L. Finn, M. H. Kryder, and C.-H. Chang, "Near-field magneto-optics and high density data storage," *Appl. Phys. Lett.*, vol. 61, no. 2, pp. 142–144, July 1992.

[11] T. J. Silva, S. Schultz, and D. Weller, "Scanning near-field optical microscope for the imaging of magnetic domains in optically opaque materials," *Appl. Phys. Lett.*, vol. 65, no. 6, pp. 658–660, Aug. 1994.

[12] E. Yamazaki, S. Wakana, M. Kishi, M. Iwanami, S. Hoshino, and M. Tsuchiya, "Three-dimensional magneto-optic near-field mapping over 10–50 mm-scale line and space circuit patterns," in *Proc. 14th Annu. Meeting IEEE Lasers Electro-Optics Society*, Nov. 2001, p. 318.

[13] T. Sudo, K. Nakano, A. Nakamura, and S. Haga, "A test chip for evaluating switching noise and radiated emission by I/O and core circuits," in *Proc. 2001 IEEE Int. Symp. Electromagnetic Compatibility*, Aug. 2001, pp. 676–680.

[14] E. Yamazaki, S. Wakana, M. Kishi, M. Tsuchiya, M. Iwanami, and S. Hoshino, "Spatial resolution evaluation of fiber edge magneto-optic probe," in *Proc. 2001 IEICE General Conf.*, vol. B-4-20, Mar. 2001, p. 335.

[15] H. Johnson and M. Graham, *High-Speed Digital Design: A Handbook of Black Magic*. Englewood Cliffs, NJ: Prentice-Hall, 1993, pp. 66–74.

[16] T. Harada, H. Sasaki, and Y. Kami, "Investigation on radiated emission characteristics of multilayer printed circuit boards," *IEICE Trans. Commun.*, vol. E80-B, no. 11, pp. 1645–1651, Nov. 1997.

[17] H. Sasaki, T. Harada, and T. Kuriyama, "A new VLSI decoupling circuit for suppressing radiated emissions from multilayer printed circuit boards," in *Proc. 2000 IEEE Int. Symp. Electromagnetic Compatibility*, Aug. 2000, pp. 157–162.

[18] J. P. Libous and D. P. O'Connor, "Measurement, modeling, and simulation of flip-chip CMOS ASIC simultaneous switching noise on a multilayer ceramic BGA," *IEEE Trans. Comp., Packag., Manufact. Technol. B*, vol. 20, pp. 266–271, Aug. 1997.

Mizuki Iwanami was born in Tochigi, Japan, in 1968. He received the B.E. degree in materials science and engineering from Waseda University, Tokyo, Japan, in 1991, and the M.E. and Ph.D. degrees in materials science from the University of Tokyo, Tokyo, Japan, in 1994 and 1997, respectively.

In 1997, he joined NEC Corporation, Kawasaki, Japan, where he was involved in research on EMI reduction techniques for printed circuit boards. In 2000, he moved to the Association of Super-Advanced Electronics Technologies (ASET), Tsukuba, Japan. He is currently engaged in research of optical near-field probing techniques and their applications to electronic devices.

Dr. Iwanami is a Member of the Institute of Electronics, Information and Communication Engineers (IEICE) of Japan.

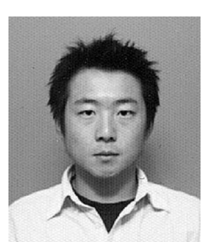

Etsushi Yamazaki was born in Toyama, Japan. He received the B.S. and M.S. degrees in electronic engineering from the University of Tokyo, Tokyo, Japan, in 2000 and 2002, respectively.

He is currently with NTT Network Innovation Laboratories, Yokosuka, Japan, where he is engaged in research on photonic transport and processing techniques.

Mr. Yamazaki is a Member of the Institute of Electronics, Information and Communication Engineers (IEICE) of Japan.

Ken Nakano was born in Aichi, Japan, in 1969. He received the B.E. and M.E. degrees in electromechanical engineering and the Ph.D. degree in electric engineering from the Nagoya University, Nagoya, Japan, in 1992, 1994, and 1997, respectively.

He joined the Mechanical Engineering Research Laboratory, Hitachi, Ltd., Tsuchiura, Ibaraki, Japan, in 1997, where he was engaged in the research and development of high-pin-count semiconductor packaging technology. He is currently a Researcher with the Tsukuba Research Center, Association of Super-Advanced Electronics Technologies (ASET), Tsukuba, Ibaraki, Japan, where he is involved in research in the field of electromagnetic compatibility with electronic system integration. His research interests include the electrical characterization of high-speed packages and wiring modules.

Dr. Nakano is a Member of the Institute of Electronics, Information and Communication Engineers (IEICE) of Japan, the Japan Institute of Electronics Packaging (JIEP), the Japan Society of Applied Physics (JSAP), and the Japan Society of Mechanical Engineers (JSME).

Toshio Sudo (A'90–SM'96) received the B.E. and M.E. degrees in electrical engineering from Tohoku University, Sendai, Japan, in 1973 and 1975, respectively.

He joined the Research and Development Center, Toshiba Corporation, Kawasaki, Japan, in 1975, where he was engaged in the research and development of high-density multichip module technology and complimentary metal–oxide–semiconductor microprocessor packaging technology. He is currently a Chief Researcher in the Microelectronics Packaging Research Center, Corporate Manufacturing Engineering Center, Toshiba Corporation. He is also a Visiting Researcher of the Association of Super-Advanced Electronics Technologies (ASET), Ibaraki, Japan, studying the large-scale-integration-level EMC reduction technique. His research interests include the electrical modeling and electrical characterization of high-speed interconnections and packages.

Mr. Sudo is a Member of the Institute of Electronics, Information and Communication Engineers (IEICE) of Japan, and IMAPS and a Senior Member of the IEEE Components Packaging and Manufacturing Technology (CPMT) Society.

Shigeki Hoshino was born in Fukuoka, Japan. He received the B. E., M.E., and Ph.D. degrees, all in physics, from Kyushu University, Japan, in 1976, 1978, and 1983, respectively.

He joined NEC Corporation, Japan, in 1983. In 1999, he moved to the Association of Super-Advanced Electronics Technologies (ASET), Ibaraki, Japan. He has been engaged in research and development of EMI reduction technologies and electromagnetic sensors.

Dr. Hoshino is a Member of the Institute of Electronics, Information and Communication Engineers (IEICE) of Japan and the Japan Society of Applied Physics.

Shinichi Wakana (M'92) was born in Tokyo, Japan, on March 13, 1959. He received the B.E. and M.E. degrees in electrical engineering from Waseda University, Tokyo, Japan, in 1982 and 1984, respectively, and has worked toward the Ph.D. degree at the University of Tokyo, Tokyo, Japan.

He has been with Fujitsu Laboratories, Ltd., Atsugi, Japan, since 1984 and was a Visiting Scholar at the University of Michigan from 1991 to 1993. He has been engaged in research and development of optical sensing technology and opto-mechatronic systems.

Mr. Wakana is a Member of the Institute of Electronics, Information and Communication Engineers (IEICE) of Japan, the Japan Society of Applied Physics, and the Optical Society of America (OSA).

Masato Kishi was born in Tokyo, Japan. He received the B.S. and M.S. degrees in physics from Nihon University in 1973 and 1975, respectively.

From 1975 to 1990, he was with the Institute of Interdisciplinary Research, formerly of the University of Tokyo, and the Research Center for Advanced Science and Technology, University of Tokyo. In 1990, he moved to the Department of Electronic Engineering in the same university. He has been involved in research projects in the fields of semiconductor material science and technology as well as in the laboratory education curriculums of the department. His current research remains focused on the advanced characterization techniques for Si and optoelectronic materials with emphasis on microscopic Raman spectroscopy and nonlinear optics/optoelectronics.

Masahiro Tsuchiya (M'97) was born in Shizuoka, Japan, on September 28, 1960. He received the B.E., M.E., and Ph.D. degrees, all in electronic engineering, from the University of Tokyo, Tokyo, Japan, in 1983, 1985, and 1988, respectively. His doctoral dissertation was on the resonant tunneling phenomena in ultrathin semiconductor heterostructures and related devices.

He was a Postdoctoral Fellow with the University of California at Santa Barbara from 1988 to 1990, and a Research Staff Member with the Research Development Corporation of Japan from 1990 to 1991. In 1991, he joined the Department of Electronic Engineering, the University of Tokyo, as a Lecturer and became an Associate Professor in the same department in 1993. From 1996 to 1997, he spent his sabbatical year as a Visiting Researcher at Bell Laboratories, AT&T/Lucent Technologies, Holmdel, NJ. In 2003, he moved to the Communications Research Laboratory, Koganei, Tokyo. His current research interests remain focused on photonics technologies for ultrafast and high-frequency systems/components, nonlinearity management, and microwave/millimeter-wave systems. He is also interested in advanced optoelectronic materials and implementations of practical optoelectronic systems with those materials.

Dr. Tsuchiya is a Member of the Japan Society of Applied Physics, the Institute of Electronics, Information and Communication Engineers (IEICE) of Japan, and the IEEE Lasers & Electro-Optics Society (LEOS).